A MINLP-based Approach for the Design-for-Control of Resilient Water Supply Systems

Aly-Joy Ulusoy, Filippo Pecci and Ivan Stoianov

***Abstract*— The improvement in resilience of water supply systems by increasing their redundancy, either in energy or in connectivity, is a common priority when doing rehabilitation and expansion. This however can come at the cost of other aspects of network performance, such as leakage management. In this work, we consider the design-for-control problem of adding new connections (from a predefined set of candidate pipes) to water supply systems to improve their resilience to failure events while minimizing the impact on leakage management under normal operating conditions. We present a mixed-integer non-linear programming formulation of the problem of optimal link addition for the minimization of average zone pressure, a surrogate measure of pressure dependent leakage. We implement a method based on spatial branch-and-bound to solve the problem on a case study network from the literature and an operational network part of an urban water system in the UK. Finally, we validate the improvement in network resilience resulting from the addition of new connections by performing an a posteriori critical link analysis, using the hydraulic resilience measure of reserve capacity.**

***Index Terms*— mixed-integer non-linear programming (MINLP), branch-and-bound (B&B) algorithm, resilience, water supply systems, Design-for-Control (DfC)**

I. Introduction

Water supply systems (WSS) represent a critical infrastructure. In their design and operation, there is significant interest in minimizing the impact on performance of failure events. Network resilience is an important factor in WSS design (and sectorization design) [1]–[9], but also in the rehabilitation and expansion of existing systems, which are the focus of this work. Resilience refers to the ability of a WSS to maintain minimum pressure levels and meet customer demand during failure events and is traditionally built in the network in the form of topological and/or energy redundancy. Energy redundancy (i.e. pressure surplus) can be provided by introducing pumps or more adaptive forms of pressure control. Improving the topological redundancy of existing WSSs, on the other hand, consists either in maintenance procedures or rehabilitation (or expansion) approaches based on link, or pipe, addition (including duplication) [7], [10]–[13].

This work was supported by the EPSRC (EP/P004229/1, Dynamically Adaptive and Resilient Water Supply Networks for a Sustainable Future), the EPSRC CDT in Sustainable Civil Engineering and Suez.

Aly-Joy Ulusoy, Filippo Pecci and Ivan Stoianov are with the Department of Civil and Environmental Engineering at Imperial College London University, London, UK (e-mails: aly-joy.ulusoy15@imperial.ac.uk; f.pecci14@imperial.ac.uk; ivan.stoianov@imperial.ac.uk).

There is no universally accepted definition or measure of resilience for WSSs, and explicitly considering resilience based on failure scenario simulations in the optimal design or rehabilitation of WSSs is complicated. Furthermore, the cost of installing new pipes aside, link addition may not always be desirable or possible in real-world systems such as WSSs: this can produce a non-feasible network model or degrade the performance of the system, in terms of pressure management for instance. Pressure management is a major challenge in the operation and management of WSSs, as it affects leakage [14] and pipe failure [15]. We present a design-for-control (DfC) approach to the problem of link addition (from a predefined set of potential candidates) to increase the resilience of WSSs while minimizing pressure throughout the network. DfC is a concurrent design process, which integrates the problem of simultaneously optimising the choice of the links to be added, and the settings of existing pressure control valves (PCV). We formulate an optimization problem, where the objective is to minimize average zone pressure (AZP) under normal operating conditions, subject to mass and energy conservation constraints, for a given number of candidate links to add.

We model water supply systems as directed graphs. Flows across links and hydraulic heads at nodes are represented by continuous variables. Binary variables are used to represent the selected (open) or un-selected (closed) state of candidate links for addition. Flow or mass conservation holds at all nodes and energy conservation constraints (also referred to as head loss or potential-flow coupling constraints [16]) are enforced along all links. Frictional head losses within pipes are described by either the Hazen-Williams or Darcy-Weisbach equations. Given the complexity of the problem of optimal WSS design and rehabilitation, most literature implements heuristic methods based on genetic algorithms (GAs) [7], [10]–[13]. However, such approaches scale badly with the size of the considered network and fail to guarantee the optimality of the computed solutions. In addition, these methods do not deal with optimal pressure control. Alternative solution approaches for DfC problems in interconnected systems rely on mathematical optimization methods. Examples include the DfC problems of optimal splitting (islanding) or expansion of power systems [17], [18], which result in the formulation of mixed-integer linear programs (MILPs). Because of the non-convexity of the potential-flow coupling constraint in WSSs, the formulation of the DfC problem of optimal link addition and pressure control results in a mixed-integer non-

linear program (MINLP), which we solve using mathematical optimization methods, as they provide a certificate of global optimality.

Previous attempts to solve MINLPs to global optimality for the design and/or control of water distribution networks use branch-and-bound methods [19]–[22]. For an introduction to mixed-integer non-linear problems and a review of methods for solving convex and non-convex MINLPs (in particular branch-and-bound), see Belotti et al. [23]. We propose to solve the problem of optimal link addition and pressure control implementing a spatial branch-and-bound (sBB) method based on the work of [22], which was shown to outperform state-of-the-art global optimization solvers for the problem of optimal valve placement in water networks. In this work, we modify the method, which generates a sequence of lower and upper bounds to the optimal value of the original problem, to include additional optimality-based bound tightening (OBBT). This further reduces the domain of the problem variables and improves the computed lower bounds compared to the algorithm presented in [22].

We solve the design-for-control (DfC) problem of optimal link addition and PCV control for two sectorised WSSs, a case-study network (Net25) and a large operational network (BWPnet), where links have been closed off with boundary valves (BV) to create isolated supply areas, called district metered areas (DMA). Permanent sectorisation is a commonly adopted practice which facilitates pressure management and leakage monitoring in WSSs but also reduces the number of independent alternative supply paths and, as a result, network tolerance to failure [24]. In sectorised WSSs, improvements in resilience can be achieved at minimal cost by reopening BVs between DMAs, as this increases the number of inlets into otherwise isolated areas. In order to preserve the benefits of network sectorisation, dynamic operation of the BVs could also be implemented, where DMAs are periodically aggregated (for improved network resilience) and segregated (for leakage monitoring) [14]. In this paper, we formulate the problem of dynamic DMA reconfiguration as an optimal link addition problem, where the set of candidate links (for addition) is defined as the set of closed BVs. We compare the implemented sBB procedure to a state-of-the-art global solver (SCIP) and show that the tailored procedure produces better feasible solutions, as well as guarantees of optimality, in all instances. We also investigate how the size of the problem affects the quality of the solution, and particularly of the final optimality gap. Finally, the improvement in network resilience resulting from the optimal addition of links in Net25 and BWPnet is validated a posteriori by carrying out a critical link analysis (CLA) on the network pipes using the measure of reserve capacity.

II. Problem Formulation

A. General problem formulation

In this paper, we consider a water supply network with n_n demand nodes or junctions, n_0 water sources (reservoirs) and n_p links (pipes or valves), among which n_{PCV} pressure control valves (PCVs) and n_{CP} candidate pipes (CPs) for addition. In the initial configuration, the CPs are all closed. In our problem formulation, the locations of the PCVs are fixed and we assume known the set of candidate pipes to be added to the network. The aim is to optimize simultaneously network design (the set of CPs to be added) and control (PCV operational settings). The length and diameter of CPs are assumed known too: if several diameters are under consideration for a given candidate location, as many candidate pipes (with different diameters) can be considered (the CPs can be mutually exclusive or not, see (9)). We model the network as a directed graph with $n_n + n_0$ vertices and n_p links. The direction of a link does not constrain the direction of flow but only defines a positive flow as directed from start to end node. Pumps are not considered in the present work and are not included in the model. We refer to V as the set of network vertices, E as the set of network links and $E_{\text{pipes}} \subset E$, $E_{\text{PCV}} \subset E$ and $E_{\text{CP}} \subset E$ the subsets of network pipes, PCVs and CPs, respectively. The vector of fixed elevations of the demand nodes is given by $\zeta \in \mathbb{R}^{n_n}$ and we consider n_t different time steps. For each time step $k = 1, \dots, n_t$, the vector of nodal demands is given by $d^k \in \mathbb{R}^{n_n}$, the (known) hydraulic heads at water sources by $h_0^k \in \mathbb{R}^{n_0}$. At time step k, we consider the continuous decision variables $h^k \in \mathbb{R}^{n_n}$ and $q^k \in \mathbb{R}^{n_p}$, representing the hydraulic heads at the network demand nodes and the vector of flow rates, respectively. Moreover, we use vector $\eta^k \in \mathbb{R}^{n_p}$ to model additional head losses introduced by the action of control valves or head differences across un-selected (closed) candidate pipes. Discrete decision variables $z \in \{0;1\}^{n_{\text{CP}}}$ represent the selected, or open (1), and un-selected, or closed (0), status of CPs. Finally, we adopt the notation $i_1 \xrightarrow{j} i_2$ to represent a link j that positively connects node i_1 (start node) to i_2 (end node).

This paper aims to investigate optimal link addition and PCV control, with the objective of improving network resilience and minimizing average zone pressure (AZP), a surrogate measure of pressure dependent leakage [14]. The objective function (AZP) is defined as a weighted sum of nodal pressures at all time steps:

$$\frac{1}{n_t W} \sum_{k=1}^{n_t} w^T (h^k - \zeta) \tag{1}$$

where $w \in \mathbb{R}^{n_n}$ and $W \in \mathbb{R}$ are the vector of AZP weights and the AZP normalization factor, respectively. For $i \in V$, we define I_i, the set of all links incident to node i. Then $w_i = \sum_{j \in I_i} \frac{L_j}{2}$ and $W = \sum_{i=1}^{n_n} w_i$, where $L \in \mathbb{R}^{n_p}$ is the vector of link lengths.

Hydraulic heads h^k, flows q^k, and additional head loss across links η^k at each time step are subject to energy and mass conservation constraints:

$$A_{12} h^k + A_{10} h_0^k + \phi(q^k) + \eta^k = 0, \quad k = 1, \dots, n_t \tag{2a}$$

$$A_{12}^T q^k - d^k = 0, \quad k = 1, \dots, n_t \tag{2b}$$

where $A_{12} \in\in \mathbb{R}^{n_p \times n_n}$ and $A_{12} \in\in \mathbb{R}^{n_p \times n_0}$ are the link node incidence matrices for the demand nodes and sources, and $\phi(q)$ is the function of friction head losses within pipes for vector of flows q.

Friction head losses are most commonly described either by the Darcy-Weisbach (D-W) or Hazen-Williams (H-W) equations. Neither formula being smooth, it is convenient to derive quadratic approximations for the D-W or H-W relationship over the operational range of flows to formulate a smooth optimization problem. Here, we compute a quadratic approximation of the H-W and D-W friction losses within each link, following the methodology presented by Eck and Mavissen [25] and based on the implementation proposed by Pecci et al. [26] for the H-W head loss model. This produces a pair of coefficients (a_j, b_j) for each link j in the network. The head loss across network link j is then given, for flow q_j^k, by $\phi_j(q_j^k) = q_j^k(a_j \left|q_j^k\right| + b_j)$ and the vector of head loss across all network links is given by $\phi(q^k) = [\phi_1(q_1^k) \dots \phi_{n_p}(q_{n_p}^k)]^T$. The resulting constraints (2a) are non-convex. To isolate the non-convex friction head loss term, we introduce the auxiliary variable $\theta^k \in \mathbb{R}^{n_p}$ and constraints (2) become:

$$A_{12}h^k + A_{10}h_0^k + \theta^k + \eta^k = 0, \quad k = 1, \dots, n_t \tag{3a}$$

$$A_{12}^T q^k - d^k = 0, \quad k = 1, \dots, n_t \tag{3b}$$

$$\theta^k = \phi(q^k), \quad k = 1, \dots, n_t \tag{3c}$$

where constraints (3) are all linear, except for the non-convex friction loss equality constraint (3c). To enforce the upper and lower bound constraints on variables q, η and θ as well as big-M constraints associated with the addition of candidate pipes, we introduce the following (constant) vectors: $h_{\min}^k$ and $h_{\max}^k \in \mathbb{R}^{n_n}$ are respectively the vectors of minimum and maximum allowed hydraulic heads at network nodes, $v^{\max} \in \mathbb{R}^{n_p}$ is the vector of maximum allowed velocities across the network links, $S \in \mathbb{R}^{n_p}$ is the vector of link cross sections defined as $S = [\pi D_1^2/4 \dots \pi D_{n_p}^2/4]^T$ where D_j is the diameter of link j , and $q^{\max} = \mathbf{diag}(S)v^{\max}$ is the corresponding vector of maximum flows across network links. Constant vectors q_U^k, q_L^k, θ_U^k, θ_L^k, η_U^k and η_L^k of upper and lower bounds on variables q, θ and η are also defined in the following way.

Both positive and negative flows (and consequently friction head losses) are allowed across network links $j \in E_{\text{pipes}}$. Flows and friction losses are only limited in absolute value by the maximum allowed velocities. We assume only friction head loss occurs across network pipes, so $\eta_j^k = 0,\ \forall j \in E_{\text{pipes}}, k = 1, \dots, n_t$. This is reflected in the upper and lower bounds on the values of q, θ and η associated with the network pipes. For all $k = 1, \dots, n_t$:

$$\begin{aligned} \forall j \in E_{\text{pipes}}, \qquad (q_U^k)_j &= q_j^{\max} \\ (q_L^k)_j &= -q_j^{\max} \\ (\theta_U^k)_j &= \phi_j(q_U^k)_j \\ (\theta_L^k)_j &= \phi_j(q_L^k)_j \\ (\eta_U^k)_j &= 0 \\ (\eta_L^k)_j &= 0 \end{aligned} \tag{4}$$

Unlike pipes, pressure control valves can only support positive flows (directed from start to end node). This constraint is also reflected by the upper and lower bounds of the friction loss and additional head loss across the valves. For all $k = 1, \dots, n_t$:

$$\begin{aligned} \forall j \in E_{\text{PCV}},\ i_1 \xrightarrow{j} i_2, \qquad (q_U^k)_j &= q_j^{\max} \\ (q_L^k)_j &= 0 \\ (\theta_U^k)_j &= \phi(q_U^k)_j \\ (\theta_L^k)_j &= 0 \\ (\eta_U^k)_j &= (h_{\max}^k)_{i_1} - (h_{\min}^k)_{i_2} \\ (\eta_L^k)_j &= 0 \end{aligned} \tag{5}$$

CPs are modeled by binary variables $z \in \{0,1\}^{n_{\text{CP}}}$. For $j = 1 \dots n_{\text{CP}}$, we refer to $l_j \in E_{\text{CP}}$ as the index of the candidate pipe modeled by the binary decision variable z_j. Then, either $z_j = 1$ and the candidate pipe l_j is selected and modeled as open link, or $z_j = 0$ and CP l_j is unselected (closed). Flow across a closed candidate pipe is forced to zero and the hydraulic heads at the start and end nodes of that link are decoupled. To enforce this, we define matrices Q_U^k, Q_L^k, Θ_U^k, Θ_L^k, N_U^k and $N_L^k \in \mathbb{R}^{n_p \times n_{\text{BV}}}$, for all $k = 1, \dots, n_t$:

$$\begin{aligned} (Q_U^k)_{ij} &= \begin{cases} q_i^{\max}, & \text{if } i = l_j \\ 0, & \text{otherwise} \end{cases} \\ Q_L^k &= -Q_U^k \end{aligned} \tag{6a}$$

$$\begin{aligned} (\Theta_U^k)_{ij} &= \begin{cases} \phi_i(q_i^{\max}), & \text{if } i = l_j \\ 0, & \text{otherwise} \end{cases} \\ \Theta_L^k &= -\Theta_U^k \end{aligned} \tag{6b}$$

$$\begin{aligned} (N_U^k)_{ij} &= \begin{cases} (h_{\max}^k)_{i_1} - (h_{\min}^k)_{i_2}, & \text{if } i = l_j,\ i_1 \xrightarrow{i} i_2 \\ 0, & \text{otherwise} \end{cases} \\ (N_L^k)_{ij} &= \begin{cases} (h_{\min}^k)_{i_1} - (h_{\max}^k)_{i_2}, & \text{if } i = l_j,\ i_1 \xrightarrow{i} i_2 \\ 0, & \text{otherwise} \end{cases} \end{aligned} \tag{6c}$$

The values of individual elements of constant vectors q_U^k, q_L^k, θ_U^k, θ_L^k, η_U^k and η_L^k for all $k = 1, \dots, n_t$ are as follows:

$$\begin{aligned} \forall j \in E_{\text{CP}},\ i_1 \xrightarrow{j} i_2, \qquad (q_U^k)_j &= 0 \\ (q_L^k)_j &= 0 \\ (\theta_U^k)_j &= 0 \\ (\theta_L^k)_j &= 0 \\ (\eta_U^k)_j &= (h_{\max}^k)_{i_1} - (h_{\min}^k)_{i_2} \\ (\eta_L^k)_j &= (h_{\min}^k)_{i_1} - (h_{\max}^k)_{i_2} \end{aligned} \tag{7}$$

Lower and upper bound constraints and big-M constraints on variables q^k, θ^k and η^k, for all $k = 1, \dots, n_t$, are given by:

$$\begin{aligned} q^k - Q_U^k z &\le q_U^k \\ -q^k - Q_L^k z &\le q_L^k \end{aligned} \tag{8a}$$

$$\begin{aligned} \theta^k - \Theta_U^k z &\le \theta_U^k \\ -\theta^k - \Theta_L^k z &\le \theta_L^k \end{aligned} \tag{8b}$$

$$\begin{aligned} \eta^k + N_U^k z &\le \eta_U^k \\ -\eta^k + N_L^k z &\le \eta_L^k \end{aligned} \tag{8c}$$

where the values of individual elements of constant vectors q_U^k, q_L^k, θ_U^k, θ_L^k, η_U^k and η_L^k are defined for links, PCVs and CPs by (4), (5) and (7) respectively, and matrices Q_U^k, Q_L^k, Θ_U^k, Θ_L^k, N_U^k and $N_L^k \in \mathbb{R}^{n_p \times n_{\text{BV}}}$ are defined by (6).

Further constraints on the sets of candidate pipes to be added can be enforced with linear inequalities on binary variables z:

$$Az \leq \mathbf{e} \tag{9}$$

where $A \in \mathbb{R}^{n_A \times n_{\text{CP}}}$ is a constant matrix of binary inequalities representing constraints on the feasible sets of candidate pipes and $\mathbf{e} \in \mathbb{R}^{n_A}$ is a n_A by 1 vector with fixed entries. The constraint can be used to prevent specific combinations of candidate pipes from being selected (e.g. duplicate pipes).

Finally, we note that, a network topology with fewer candidate pipe additions could result in lower AZP values. As a result, minimizing AZP could produce not necessarily resilient network structures, with the addition of few candidate pipes. To ensure that the solution of the problem minimizes AZP while adding new connections, the number of pipes to add is fixed to n_b:

$$\mathbb{1}_{n_{\text{CP}}} z = n_b \tag{10}$$

The problem of minimizing (1), subject to (3a)-(3c), (8a)-(8c), (9) and (10) results in a non-convex mixed-integer non-linear program (MINLP):

$$\begin{aligned}
\underset{z,q,h,\eta,\theta}{\text{minimize}} \quad & \frac{1}{n_t W} \sum_{k=1}^{n_t} w^T (h^k - \zeta) \quad \text{(AZP)} \\
\text{subject to} \quad & A_{12} h^k + A_{10} h_0^k + \theta^k + \eta^k = 0, \\
& A_{12}^T q^k - d^k = 0, \\
& \theta^k = \phi(q^k), \\
& q^k - Q_U^k z \leq q_U^k, \\
& -q^k - Q_L^k z \leq q_L^k, \\
& \theta^k - \Theta_U^k z \leq \theta_U^k, \\
& -\theta^k - \Theta_L^k z \leq \theta_L^k, \\
& \eta^k + N_U^k z \leq \eta_U^k, \\
& -\eta^k + N_L^k z \leq \eta_L^k, \\
& \mathbb{1}_{n_{\text{CP}}} z = n_b, \\
& Az \leq \mathbf{e}, \\
& z \in \{0;1\}^{n_{\text{CP}}}, \\
& q^k \in \mathbb{R}^{n_p}, h^k \in \mathbb{R}^{n_n}, \eta^k \in \mathbb{R}^{n_p}, \theta^k \in \mathbb{R}^{n_p}, \\
& \forall k \in \{1, ..., n_t\},
\end{aligned} \tag{11}$$

where $q = (q^k)_{k=1,...,n_t}$, $h = (h^k)_{k=1,...,n_t}$, $\eta = (\eta^k)_{k=1,...,n_t}$ and $\theta = (\theta^k)_{k=1,...,n_t}$.

B. Sectorised WSS

In the case of sectorised WSSs, where boundary valves (BVs) have been installed to shut off connections and create isolated supply sectors (DMAs), new links can be added to the network by reopening closed BVs. Since the cost of opening BVs is minimal compared to installing new pipes, as a first step in the enhancement of resilience of sectorised WSS, we restrict the set of candidate pipes for addition E_{CP} to the set $E_{\text{BV}} \subset E$ of closed BVs between DMAs and investigate DMA aggregation solutions to improve network resilience. However, following the necessity to preserve the sectorised structure of the network for leakage management purposes, DMA aggregation is restricted to pairing: each DMA can only be paired with at most one other DMA, so the pairing of two DMAs excludes pairing opportunities with other DMAs. The pairing constraint is enforced with (9), where $A \in \mathbb{R}^{n_A \times n_{\text{BV}}}$ is the constant matrix of binary inequalities representing DMA coupling constraints and $\mathbf{e} = \mathbb{1}_{n_A}$, the n_A by 1 vector with all entries 1. For the details of the computation of matrix A, see Appendix I.

III. Solution Method

Problem (11) is a non-convex MINLP, combining integer decision variables, non-linear and non-convex functions into a computationally intensive NP-hard problem. One approach to tackle non-convexity is to use (linear) convex hull relaxations or piecewise linear approximations, which can be reformulated into linear constraints and handled by MILP solvers. Ultimately, this method does not solve the original MINLP but an approximation of the problem, and does not necessarily produce a feasible solution. A common approach for directly solving non-convex MINLPs is spatial branch-and-bound (sBB) [23], [27]: the original problem is recursively divided into subproblems with increasingly smaller feasible sets and lower bounds on the solution of the subproblems are computed using convex relaxations of the non-convex functions to produce a certificate of optimality.

The sBB methods adopted in this paper (presented in Figure 1) to solve the problem of optimal link addition and pressure control are based on the work of Pecci et al. [22], who attempt to solve the problem of optimal valve placement and control in water supply networks. In Section III-A we provide a brief overview of the different stages involved in the procedure implemented by [22], that we refer to as BB_0. To improve the performance of their algorithm, Pecci et al. implement a preliminary domain reduction (bound tightening) step, described in Section III-B. Domain reduction allows to produce tighter MILP relaxations and, as a result, better lower bounds to the optimal value of the MINLP [28]. Here, we expand the algorithm from [22] and implement a modified method, referred to as $\text{BB}_{\text{BT+}}$, where the domain of the variables of the subproblems are reduced at each branch-and-bound iteration. This results, as we show in the analysis of the networks Net25 and BWPnet (see Section IV-A and IV-B, Figures 3 and 6), in better solutions and tighter optimality gaps than those obtained by solving MINLP (11) with BB_0. The procedures of the implemented branch and bound methods are summarised in Figure 1.

Finally, Section III-C describes an a posteriori critical link analysis (CLA) based on the measure of reserve capacity that is applied in this work to validate the improvement in resilience of the optimal system configurations produced by solving MINLP (11).

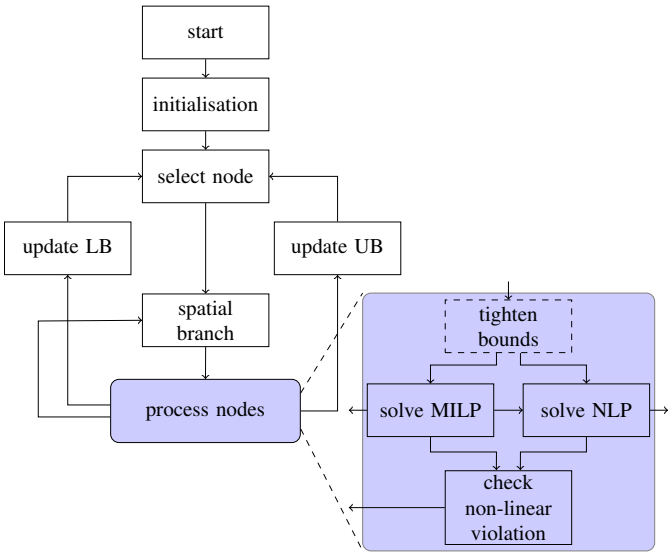

Fig. 1. BB_0 procedure, based on Pecci et al. [22]. BB_{BT+} is obtained by including the dashed outline box (tighten bounds).

A. Branch-and bound procedure

1) Bounding strategy: We compute a polyhedral envelope of the potential-flow coupling constraint (3c) implementing a method developed by Liberti and Pantalides [29] for monomials of odd degree, and since all other constraints (and objective function) in MINLP (11) are linear, MINLP (11) is relaxed to a MILP. The relaxed MILP is then solved using standard (integer) branch-and-bound methods (i.e. integer search tree). In practice, the solution of the relaxed problem is rarely feasible, but its optimal value provides a lower bound on the optimal value of the original MINLP. We then fix the binary variables in MINLP (11) to the values obtained from the solution of the MILP relaxation. If feasible, the resulting (non-convex) nonlinear program (NLP) is solved using a gradient-based NLP solver to produce a local optimum, providing an upper bound to the optimal value of the original problem.

2) Branching strategy: Spatial branching is carried out in the branch-and-bound procedure by partitioning selected problems into descendant subproblems. For MINLP (11), tighter relaxations of the head loss constraints are produced, at each iteration, by branching on the flow variables of the problem: the feasible set is split into two, creating two subproblems with tighter variable bounds. This allows to compute increasingly better lower bounds. Details of the implemented bounding and branching strategies can be found in [22].

B. Bound tightening

Bound tightening consists in reducing the domain of the variables of a problem, taking into account bounds on other variables and the problem constraints. In particular, for MINLP (11), an Optimality-Based Bound Tightening (OBBT) method based on [22] is implemented to tighten the bounds on flow and frictional head loss variables and, as a result, the relaxations of the head loss constraints in the MILP. Tighter bounds are computed by maximizing and minimizing in turn the flow variables q_i subject to a linear relaxation of the constraints of MINLP (11). In particular, integrality constraints on the binary variables z are relaxed and, as for the computation of the lower bound, potential-flow coupling constraints (3c) are linearized using a polyhedral relaxation. A linear relaxation of the constraints produces weaker bounds than a non-linear convex relaxation but can be solved more efficiently. OBBT methods are still, in general, computationally intensive (especially for large problems) and are often limited to the pre-processing stage [22] and/or early branch-and-bound iterations [28].

OBBT however allows to reduce the feasible sets of the subproblems in the branch and bound search tree much more efficiently than branching alone and previous studies have shown that, in some cases, there is a benefit to applying tightening methods throughout the search [30]. For this reason, we suggest implementing additional OBBT steps throughout the sBB procedure (see Figure 1). The resulting branch-and-bound procedure (including the iterative bound tightening steps) is referred to as BB_{BT+}. The computational overhead associated with the additional bound tightening steps is expected to affect the performance of BB_{BT+}. In Section IV, we apply BB_{BT+} to the solution of optimal DMA pairing in BWPnet, and we discuss a practical method based on network reduction to apply BB_{BT+} to optimization problems formulated for large scale water systems. In Section IV, we apply both BB_0 and BB_{BT+} to solve MINLP (11) for systems Net25 and BWPnet. We compare the results of the two algorithms and comment on the impact of additional bound tightening on the performance of BB_{BT+}.

C. Resilience analysis

In order to evaluate the impact of link additions on system resilience, we perform an a posteriori analysis of the configuration solutions of MINLP (11) using a critical link analysis (CLA) and reserve capacity as a measure of individual link criticality.

Common approaches for the analysis of water system resilience use either surrogate indices, such as Todini's resilience index [31] or the statistical network entropy [32], or simulation-based criticality analyses - for an exhaustive review of resilience indices for WSSs, see [33] and [8]. Surrogate indices, which measure the topological and/or energy redundancy of WSS, are either based on the hydraulic properties under normal operation, which might not hold under failure conditions, or do not account for the hydraulic properties of the system at all. In comparison, a critical link analysis (CLA) allows to assess the criticality of each link individually, based on hydraulic simulations under failure scenarios. This provides more insight into local resilience issues that can arise due to the WSS topology. For the CLA, the PCV settings are not fixed so as to minimize AZP, as we do not consider normal system operating conditions. In this work, we carry out a CLA: individual link failures are simulated one by one and the reserve capacity (rc) of the resulting WSS configurations is computed as a measure of criticality of the failed link.

Reserve capacity is a well established measure of transportation network resilience and was adapted to water supply

systems in [34] and in [35] under the name of residual capacity. The reserve capacity of a WSS is defined as the maximum feasible demand multiplier, i.e. the maximum multiplier that can be applied to system demands without resulting in violations of the minimum pressure service levels. It assesses the hydraulic resilience of a WSS (i.e. tolerance to increase in demands) under mechanical failure conditions (i.e. failure of system components) [36], [37]. A unique demand multiplier is considered for all demand nodes, which means that if an individual pipe failure leads to the isolation of one or more customer nodes, the reserve capacity of the system drops to 0. A reserve capacity value of less than 1 means the system is able to meet only a fraction of the demand associated with at least one node, whereas a reserve capacity value greater than or equal to 1 means the system is able to meet the demands at all nodes. For more details about reserve capacity, as well as the methodology for computing the measure and carrying out the CLA, see [34].

IV. Results and Discussion

In this work, we solve the problem of optimal link addition and PCV control for two sectorised WSSs. We define the set of candidate links for addition as the set of closed BVs at the boundary between the WSSs DMAs. For operational (i.e. leakage management) purposes, we constrain the addition of new pipes (opening of BVs) to limit DMA aggregation to pairing, as described in Section II-B.

The spatial branch-and-bound (sBB) procedures BB_0 and BB_{BT+} presented in Section III are implemented in Matlab 2018b-64 bit for Windows. Relaxed MILPs within the sBB algorithms as well as the $2n_p$ LPs of the OBBT step are solved using gurobi (v8.1) [38]. NLPs are solved by IPOPT (v3.12.9) [39] using the Matlab interface [40]. To take advantage of the sparse structure of the NLPs, the pre-computed sparse gradients and Jacobians are directly provided to the solver.

MINLP (11) is also solved directly by calling the state-of-the-art global MINLP solver SCIP, to assess the performance and validate the results of the tailored branch-and-bound procedures BB_0 and BB_{BT+}. The SCIP Optimization Suite (v6.0) [41] was implemented in Matlab, via the OPTI toolbox interface. SCIP also implements a spatial branch-and-bound approach. Similarly to BB_{BT+}, SCIP performs additional bound tightening on selected subproblems within the branch-and-bound procedure [27]. Unlike the sBB procedures BB_0 and BB_{BT+} however, SCIP produces lower bounds on the solution of the original problem by solving a convex continuous relaxation of the MINLP subproblems in the branch-and-bound tree: non-convex constraints are relaxed using a convex or polyhedral envelope and integrality constraints are ignored.

Finally, we analyse the optimal system topologies obtained by solving MINLP (11) and validate the achieved improvement in resilience with a CLA using reserve capacity.

A. Case study 1: Net25

To demonstrate the implemented branch-and-bound methods, we modify a case study network from the literature, Net25, to include BVs and PCVs. For the purpose of this problem, we also assume all nodes with positive demand to be DMAs. The edited Net25 (see Figure 2) is a WSS comprising 3 reservoirs, 16 nodes (among which 8 DMA nodes with positive demand), and 26 links (15 pipes, 3 PCVs and closed 8 BVs). Friction head losses across network links are modelled using the H-W equation, and 24 time steps are considered. This results in a MINLP with 1656 continuous variables, 8 binary variables, 2934 linear constraints and 624 non-linear constraints.

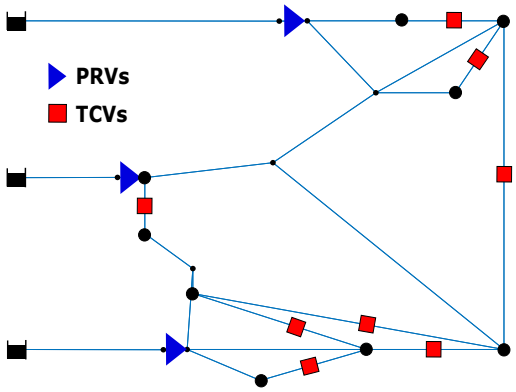

Fig. 2. Example network model Net25: Pressure control valves are represented in blue and boundary valves in red.

t (s)	n_b	Iterations	LB (m)	UB (m)	gap (%)
14,400	1	2088	14.2	18.3	29
14,400	2	3809	14.0	18.3	31
14,400	3	4757	14.0	19.8	41
14,400	4	8574	18.3	19.9	9

TABLE I
SOLUTIONS OF MINLP (11) OBTAINED WITH BB_0, WITH $n_b = 1, 2, 3, 4$ FOR NET25 (RUNNING TIME IS 4 HOURS). THE RELATIVE OPTIMALITY GAP IS DEFINED AS $\frac{UB-LB}{LB}$.

Based on hydraulic simulations of the original network, the maximum allowed velocity is fixed to 2m/s for all network pipes and a (smooth) quadratic approximation $\phi(\cdot)$ of the Hazen-Williams formula is adopted to model head loss across the pipes, as proposed in [22] and [26]. The pressure requirement at customer nodes (i.e. network nodes with strictly positive demand) is fixed to 15m. We solve MINLP (11) in Net25 with BB_0, BB_{BT+} and SCIP for different values of n_b ranging between 1 and 4 (which is the maximum number of boundary valves that can be simultaneously opened without violating the DMA pairing constraint). The maximum running time is set to 14,400s (4h). The results are summarised by Figure 3, Tables I, II and III. Below, we comment on the results, as well as the performance of the individual components of the implemented sBB algorithm.

1) Solution of the MINLP: The (feasible) solutions produced by BB_0 and BB_{BT+} have better objective value than the solutions produced by SCIP, for all values of n_b (Tables I, II, III). The objective values of the solutions produced by BB_0 and BB_{BT+} differ by less than 1% (Tables I and II). Furthermore, both BB_0 and BB_{BT+} find a good feasible solution after only a few steps of the branch-and-bound procedure. This confirms

t (s)	n_b	Iterations	LB (m)	UB (m)	gap (%)
14,400	1	1,022	16.9	18.2	8
14,400	2	983	16.6	18.2	10
14,400	3	999	17.2	19.8	15
14,400	4	1,006	19.2	19.9	4

TABLE II

SOLUTIONS OF MINLP (11) OBTAINED WITH $\text{BB}_{\text{BT+}}$, WITH $\boldsymbol{n_b = 1, 2, 3, 4}$ FOR NET25 (RUNNING TIME IS 4 HOURS). THE RELATIVE OPTIMALITY GAP IS DEFINED AS $\frac{\text{UB}-\text{LB}}{\text{LB}}$.

t (s)	n_b	Iterations	LB (m)	UB (m)	gap (%)
14,400	1	-	10.8	18.5	71
14,400	2	-	7.6	20.0	163
14,400	3	-	7.0	20.0	186
14,400	4	-	11.1	20.6	86

TABLE III

SOLUTIONS OF MINLP (11) OBTAINED WITH SCIP, WITH $\boldsymbol{n_b = 1, 2, 3, 4}$ FOR NET25 (RUNNING TIME IS 4 HOURS). THE RELATIVE OPTIMALITY GAP IS DEFINED AS $\frac{\text{UB}-\text{LB}}{\text{LB}}$.

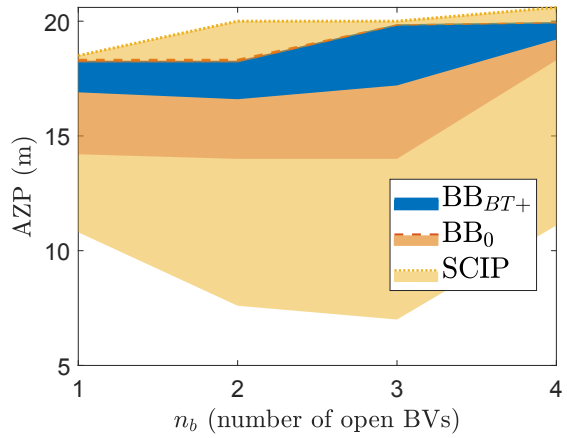

Fig. 3. Results (upper, lower bounds and optimality gaps) of MINLP (11) obtained for Net25 with BB_0, $\text{BT}_{\text{BT+}}$ and SCIP, for $\boldsymbol{n_b = 1, 2, 3, 4}$.

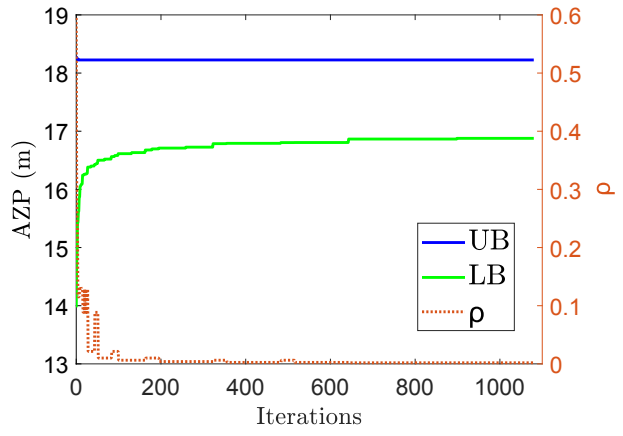

Fig. 4. Results of $\text{BB}_{\text{BT+}}$ in Net25 for $\boldsymbol{n_b = 1}$. ρ represents the reduction in the diameter of the intervals of the flow variables (defined as $\textbf{diam} = \max_{k,j}((q_U^k)_j - (q_L^k)_j)$) achieved with OBBT.

the observations made in [22]: good progress on the upper bound is made in the early stages of the execution of the branch-and-bound algorithm, i.e. a good quality feasible (if not optimal) solution is found fast. Subsequent steps mainly consist in improving the lower bound on the optimal value of MINLP (11).

The final optimality gaps returned by $\text{BB}_{\text{BT+}}$ range between 3.6% and 13% (Table II), i.e. about half to a third of the gaps returned by BB_0 (see Table I) and a tenth of the gaps returned by SCIP (see Table III). This is likely to be due to faster progress on the lower bound, resulting from the solution of tighter linear relaxations in $\text{BB}_{\text{BT+}}$. The wider the bounds on flow variable q, the wider the range of head loss values around $\phi(q)$ is allowed by the relaxations of constraints (3c). The iterative refining of the relaxations in BB_0 (past the initial iteration) follows from branching alone, whereas, in $\text{BB}_{\text{BT+}}$, additional OBBT steps allow to further refine the bounds of the flow variables q and the relaxations of the head loss constraints: Figure 4 shows that ρ, which measures the reduction in the range of flow variables achieved with OBBT, is still close to 0.1 (i.e. 10% reduction on the interval range) after 50 iterations. These results demonstrate the benefit of implementing iterative bound tightening within the sBB procedure. Furthermore, Figure 4 shows that the slow down in the progress on the lower bounds coincides with the decline of ρ, suggesting that the limit of OBBT has been reached. Like $\text{BB}_{\text{BT+}}$, SCIP also implements iterative bound tightening steps. The relaxed problems solved by SCIP to produce the lower bounds on the optimal value of MINLP (11) however drop the integrality constraints on variables z: the obtained LP relaxations are not as tight as the MILP relaxations in $\text{BB}_{\text{BT+}}$, resulting in larger optimality gaps (Tables II and III).

In conclusion, the tailored sBB methods find better feasible solutions of MINLP (11) than SCIP in Net25 for all values of $n_b = 1, \ldots, 4$. Better guarantees of optimality on the optimal solutions are produced with $\text{BB}_{\text{BT+}}$ compared to BB_0, despite an average 79% decrease in the total number of branch-and-bound iterations resulting from the computational overhead of OBBT. The quality of the final optimality gap depends on the tightness of the relaxed problems solved to produce the lower bounds, not the total number of branch-and-bound iterations.

2) Network AZP: Figure 3 shows that, overall, the optimal AZP of Net25 increases with n_b, from 18.2 m when $n_b = 1$, to 19.9 m when $n_b = 4$, when the maximum number of new links is reached. In comparison, the optimal average AZP value achieved in the sectorised configuration is 18.2 m. These results suggest that, for the considered case study, AZP minimization and resilience (measured by the surrogate measure n_b in the optimization problem) maximization are conflicting objectives of MINLP (11).

3) Network resilience and link criticality: In this section, we further analyse the resilience of the solutions of MINLP (11) obtained for $n_b = 1, \ldots, 4$ using reserve capacity and comment on the trade-off between AZP and network resilience in Net25. A summary of the results of the CLAs is provided in Figure 5, which represents the box-plot of reserve capacity values associated with the failure of individual links in Net25 for optimal DMA pairing configurations found by solving

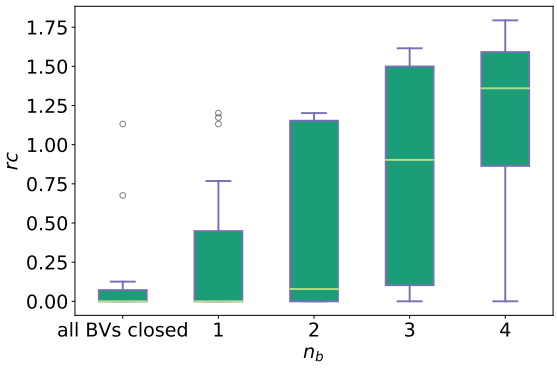

Fig. 5. Box-plot of reserve capacity (rc) associated with the failure of individual links in Net25 configurations obtained for $\boldsymbol{n_b = 1, \ldots, 4}$. The circle markers represent outliers.

MINLP (11) for $n_b = 1, \ldots, 4$. We also represent on Figure 5 the results of the CLA performed on the original configuration of Net25 (all BVs closed).

Originally, the reserve capacity of 87% of Net25 pipes is less than or equal to 0.13, and it is equal to 0 for over half the pipes in Net25. Single pipe failure events affect the ability of Net25 to meet even a fraction of nominal customer demand in the sectorised configuration. This is due to the tree-like configuration of Net25: as the original configuration of Net25 features no loops, most pipes are on exclusive supply paths. The number of sources provides some redundancy, but the network is able to supply only a fraction of the nominal demand when it has to rely on 2 reservoirs instead of 3.

We observe on Figure 5 that the reserve capacity of pipes in Net25 increases with the number of open BVs (n_b) in the network configuration: the interquartile range of reserve capacity values ranges from 0 to 0.45 for $n_b = 1$, 0 to 1.15 for $n_b = 2$, 0.1 to 1.5 for $n_b = 3$, and finally 0.86 to 1.6 for $n_b = 4$, when the maximum number of boundary valves are opened. In Net25, the addition of new links between DMAs (i.e. the opening of boundary valves), even under pairing constraints, leads to a significant increase in the reserve capacity of the network for a minor increase in network AZP: for $n_b = 4$, two thirds of all Net25 pipes are associated with a reserve capacity value greater than or equal to 1 (i.e. their individual failure does not impact the ability of the network to supply customer nodes under normal demand conditions), compared to only one pipe in the sectorised configuration, for less than a 7% increase in AZP. This can help mitigate the effect of individual pipe failure events and increases the resilience of the network.

4) 24-hour optimization vs. peak demand: Finally, we solve MINLP (11) in Net25 for a single time step, at peak demand, for all values of $n_b = 1, \ldots, 4$. This results in a problem with 69 continuous variables, 8 binary variables, 151 linear constraints and 26 non-linear constraints. The running time is set to 180s (3min). The results of the optimization problem are reported in Table IV, for all values of $n_b = 1, \ldots, 4$. We refer to the binary solutions of MINLP (11) at peak demand (time step 10) for different values of $n_b = 1, \ldots, 4$ as $z^{10}_{n_b}$.

t (s)	n_b	LB_{10} (m)	UB_{10} (m)	AZP_{24} (m)
180	1	17.2	17.2	18.2
180	2	17.2	17.2	18.2
180	3	18.6	18.6	19.6
180	4	19.4	19.4	19.9

TABLE IV
SOLUTION OF MINLP (11) COMPUTED WITH BB_{BT+} FOR NET25 OVER A SINGLE TIME STEP (PEAK DEMAND) AND OPTIMAL AZP (M) VALUES OBTAINED FOR CONFIGURATIONS $\boldsymbol{z^{10}_{n_b}}$, WITH $\boldsymbol{n_b = 1, 2, 3, 4}$, OVER ALL TIME STEPS

For all values of $n_b = 1, \ldots, 4$, we then fix the binary variables z in MINLP (11) to $z^{10}_{n_b}$ and we solve the resulting (continuous) non-convex program (with IPOPT) to compute AZP_{24}, the minimal average AZP values over all time steps corresponding to configurations $z^{10}_{n_b}$. The obtained local minima are recorded, for $n_b = 1, \ldots, 4$, under AZP_{24} in Table IV. We compare the results to the values in Table II, the objective values of the solutions to problem (11) solved for all time steps on Net25.

Table IV shows that AZP values AZP_{24} are, for all values of $n_b = 1, \ldots, 4$, less than or equal to the optimal AZP values found by solving MINLP (11) for Net25 over all times steps. For Net25, solving MINLP (11) at peak demand, and not over all time steps, does not result in suboptimal pairing configurations but instead produces at least as good solutions than solving MINLP (11) for Net25 over all time steps.

We observe that the number of unknowns and constraints in MINLP (11) grows rapidly with the number of time steps, and the number of pipes and nodes included in the considered water network. Therefore, when large operational networks and multiple time steps are considered, the computational cost required to solve the resulting mixed inter nonlinear program could be impractical. Results reported in Table IV suggest that MINLP (11) can be solved over a single time step (peak demand), without affecting the quality of the computed solutions.

B. Case study 2: BWPnet

The problem formulation is also applied to the optimization of the design and control of BWPnet, an operational network which is part of an urban water system in the UK. For BWPnet, the Darcy-Weisbach (DW) model of friction head loss across the network pipes is adopted and a maximum allowed velocity of 3 m/s is fixed for all pipes. The network counts 10099 nodes and 4 sources for 10597 links, among which 21 are PCVs and 57 are BVs. A 15-minute resolution daily demand pattern is available for BWPnet, which represents 96 time steps in total over 24h. The resulting MINLP has over 3 million continuous variables, 57 binary variables, over 5 million linear constraints and 1 million non-linear constraints.

1) Model reduction: The complexity of the optimization problem grows with the size of the network. In particular, the more links in the network, the more non-convex constraints in MINLP (13) and the more branching steps we expect the branch-and-bound algorithm will require to converge. The results of the analysis of Net25 show that loose bounds on flow and head loss variables q and θ in the MILP result in slower

progress on the lower bound and larger final optimality gap (see Section IV-A). Furthermore, OBBT is too computationally intensive to be applied within the branch-and-bound algorithm for large networks (BWPnet is over two orders of magnitude larger than Net25). To address these limitations and solve MINLP (13) for BWPnet, we extract a reduced model of the network. We implement the skeletonization procedure described in [42], based on the removal of branching pipes, and substitution of pipes in series and parallel pipes with pseudolinks. Nodal demands and minimum pressure requirements are adjusted to account for the properties of the removed system parts, together with pseudolink characteristics. However, the reduced model is not equivalent to the original network.

We apply the model reduction procedure to BWPnet, excluding PCVs and BVs from the set of links to be removed. We also limit the optimization problem to a single time step. We consider the demand conditions of the network at peak demand, as this provides good (if not optimal) solutions for Net25 (see Tables II and IV). In conclusion the formulation of MINLP (13) results in a problem with 4136 continuous variables, 57 binary variables, 9787 linear constraints and 1511 non-linear constraints.

2) $\mathrm{n_b}$*:* We solve the problem of optimal DMA pairing in BWPnet for different numbers of BVs n_b to open, to investigate the trade-off between resilience and AZP. To find the maximum (feasible) value of n_b, we solve the following MILP, which maximizes the number of open BVs subject only to the pairing constraints in BWPnet:

$$\begin{aligned} \underset{z}{\text{maximize}} \quad & \mathbb{1}_{n_{\mathrm{BV}}} z \\ \text{subject to} \quad & Az \leq \mathbb{1}_{n_A} \\ & z \in \{0;1\}^{n_{\mathrm{BV}}} \end{aligned} \tag{12}$$

where the binary variables z represent the open or closed state of the BVs in the network. Based on the solution of MILP (12), we find that feasible values of n_b for BWPnet range from 0 (i.e. the original sectorised network configuration) to 25. Due to the large range of values (and size of the optimization problem), we do not consider all values between 0 and 25 but instead we solve the following MINLP for $n_b = 5, 10, 15, 20, 25$:

$$\begin{aligned} \underset{z,q,h,\eta,\theta}{\text{minimize}} \quad & \frac{1}{n_t W} \sum_{k=1}^{n_t} w^T (h^k - \zeta) \quad \text{(AZP)} \\ \text{subject to} \quad & \mathbb{1}_{n_{\mathrm{BV}}} z \geq n_b, \\ & Az \leq \mathbb{1}_A, \\ & z \in \{0;1\}^{n_{\mathrm{BV}}}, \\ & (q^k, h^k, \eta^k, \theta^k) \in \mathrm{F}_z^k, \\ & \forall k \in \{1, ..., n_t\} \end{aligned} \tag{13}$$

where $\mathrm{F}_z^k \subset \mathbb{R}^{n_p} \times \mathbb{R}^{n_n} \times \mathbb{R}^{n_p} \times \mathbb{R}^{n_p}$ is the set defined by (3a)-(3c) and (8a)-(8c), $\forall k \in \{1, ..., n_t\}$. The equality constraint on the number of open BVs in MINLP (11) is replaced by an inequality: instead of solving MINLP (11) for all values of $n_b \in [1; 25]$, we define a lower bound on the number of BVs to open in MINLP (13) and allow for $\mathbb{1}_{n_{\mathrm{BV}}} z$ to take all values in the integer intervals $[n_b; 25]$.

t (s)	n_b	Iterations	LB (m)	UB (m)	gap (%)
86,400	5	581	25.1	31.9	27
86,400	10	536	25.1	31.4	25
86,400	15	680	25.1	31.3	25
86,400	20	1078	25.5	31.8	25
86,400	25	2054	30.3	36.1	17

TABLE V

SOLUTION OF MINLP (13) ON THE REDUCED MODEL OF BWPNET WITH $\mathrm{BB_0}$, FOR $\boldsymbol{n_b = 5, 10, 15, 20, 25}$, AT PEAK DEMAND. THE RELATIVE OPTIMALITY GAP IS DEFINED AS $\frac{\mathrm{UB-LB}}{\mathrm{LB}}$.

t (s)	n_b	Iterations	LB (m)	UB (m)	gap (%)
86,400	5	37	27.4	30.7	12
86,400	10	36	27.4	31.1	13
86,400	15	29	27.5	31.3	14
86,400	20	33	28.3	31.8	12
86,400	25	24	33.6	36.1	7

TABLE VI

SOLUTION OF MINLP (13) ON THE REDUCED MODEL OF BWPNET WITH $\mathrm{BB_{BT+}}$, FOR $\boldsymbol{n_b = 5, 10, 15, 20, 25}$, AT PEAK DEMAND. THE RELATIVE OPTIMALITY GAP IS DEFINED AS $\frac{\mathrm{UB-LB}}{\mathrm{LB}}$.

3) Solution of the MINLP: As for Net25, we solve MINLP (13) for the reduced model of BWPnet with $\mathrm{BB_0}$, $\mathrm{BB_{BT+}}$ and SCIP. Given the size of the problem, the running time is set to 86400 s (1 day). SCIP is not able to produce a solution in one day of computation for any value of n_b. We comment on the solutions of MINLP (13) obtained with $\mathrm{BB_0}$ and $\mathrm{BB_{BT+}}$ for $n_b = 5, 10, 15, 20, 25$, summarised in Tables V and VI and Figure 6, and analyse the impact of the individual steps of BB and $\mathrm{BB_{BT+}}$ on the overall performance of the tailored procedures.

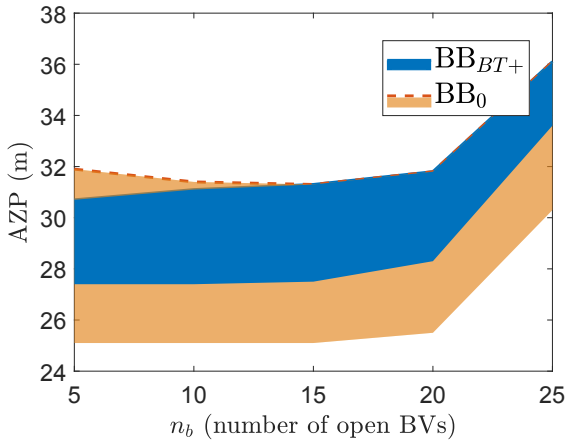

Fig. 6. Results (upper, lower bounds and optimality gaps) of $\mathrm{BB_0}$ and $\mathrm{BB_{BT+}}$ in BWPnet for different values of $\boldsymbol{n_b}$ (minimum number of boundary valves opened) ranging from 5 to 25, in steps of 5. SCIP was not able to produce a feasible solution within the time limit (1 day).

The optimal values found for $n_b = 5, 10, 15, 20, 25$ with $\mathrm{BB_0}$ and $\mathrm{BB_{BT+}}$ are similar, if not identical (e.g. for $n_b = 15, 20, 25$) - see Tables V and VI. Furthermore, good (if not optimal) solutions are found early in the branch-and-bound procedure. Subsequent steps mostly consist in tightening the optimality gap by improving the lower bound. This seems to confirm the conclusions drawn from the analysis of Net25:

the upper bounding strategy is able to provide a good incumbent solution after a small number of branch-and-bound iterations and its performance does not seem to depend on the implementation of additional bound tightening steps. As for Net25 however, BB_{BT+} (Table VI) produces better optimality gaps for BWPnet than BB_0 (Table V): the optimality gaps obtained for the solution of MINLP (13) with BB_0 are about twice as wide, on average, than the optimality gaps obtained with BB_{BT+}. Once again, the tighter relaxations produced by OBBT seem to outweigh the computational overhead of implementing the method at each branch-and-bound iteration. The final relative optimality gaps obtained with BB_{BT+} remain large (12% on average), due to an early slow-down in the progress of the lower bound. The absolute optimality gaps (3.4 m on average), although larger than the optimality gaps obtained for Net25 (Table II), are still of the same order of magnitude as the uncertainty that is likely to affect pressure control in operational networks of this size (as a result of the stochasticity of customer demand and discrepancies in the hydraulic model) [14], [22].

In conclusion, for BWPnet, as for Net25, the tailored sBB procedure BB_{BT+} performs the best: for all values of $n_b = 5, 10, 15, 20, 25$, it produces equivalent or better feasible solutions and optimality gaps than BB_0. In both case studies, and for all values of n_b considered, the tighter relaxations produced by OBBT seem to outweigh the computational overhead of implementing the method at each branch-and-bound iteration. Finally, we were not able to compare the performance of BB and BB_{BT+} to SCIP on the operational network model BWPnet, as the state-of-the-art solver could not produce a feasible solution within the time limit of one day.

4) Network AZP: The optimal AZP of the reduced BWPnet network increases with n_b, from 30.7 m when $n_b = 5$ to 36.1 m when $n_b = 25$, i.e. when the maximum number of BVs are open (see Figure 6). Figure 6 however shows that there is a jump in AZP values between $n_b = 20$ and $n_b = 25$. When going from $n_b = 5$ to $n_b = 20$, which results in a difference in configurations of 15 additional links, optimal network AZP varies by little more than 1 m, reaching a maximum of 31.8 m for $n_b = 20$, which represents a 2.6 m increase in AZP compared to the original sectorised configuration. This suggests that, although AZP minimization and link addition are conflicting objectives for the considered case study, improvement in network resilience could be achieved for a reasonable increase in AZP.

5) Network resilience and link criticality: We assess the improvement in resilience achieved in BWPnet resulting from the addition of new links. A summary of the results is provided in Figure 7, which represents a histogram of the number of links with reserve capacity greater than 1 in the optimal DMA configurations found by solving MINLP (13) for $n_b = 5, 10, 15, 20, 25$. We compare the results against a CLA of the baseline sectorised configuration. We use the rc value threshold of 1, as a reserve capacity greater than 1 means the system is able to meet customer demands in the presence of pipe failure. Alternatively, other rc thresholds can be used for the analysis (e.g. if partial customer supply is tolerated under failure conditions).

In the original (sectorised) network configuration, 5450 pipes have a reserve capacity value greater than 1. This number increases with n_b, to 6113 (representing a 12% increase in the number of pipes associated with a reserve capacity value greater than 1) for $n_b = 25$ (see Figure 7): the opening of $n_b = 25$ BVs allows to meet nominal customer demand under 663 more individual pipe failure scenarios. As for Net25, the addition of links to BWPnet also results in a general increase in the reserve capacity of BWPnet pipes: the median and average reserve capacity values increase from 4.48 and 3.62 for $n_b = 5$ to 5.47 and 4.95 respectively for $n_b = 25$. For $n_b = 5, 10, 15, 20, 25$, most BWPnet pipes have similar reserve capacity values (rc), resulting in very narrow interquartile ranges centered around the increasing median rc value.

Solving MINLP (13) for $n_b = 5, 10, 15, 20, 25$ results in the creation of respectively 2, 3, 3, 4 and 5 DMA pairs in BWPnet. The addition of links between DMAs under the constraint of pairing allows to increase the network reserve capacity associated with individual link failures and, as a result, reduces the risk of interruption of supply, by providing alternative DMA inlets and supply routes to customer nodes. More resilient structures could be achieved by removing the pairing constraints and adding more links (i.e. opening more BVs). However, this would not necessarily produce a feasible network configuration: opening all 57 BVs in BWPnet, for instance, results in a hydraulically infeasible network model. Furthermore, this would result in the loss of the sectorized network structure and, consequently, an increase in pressure management implementation complexity.

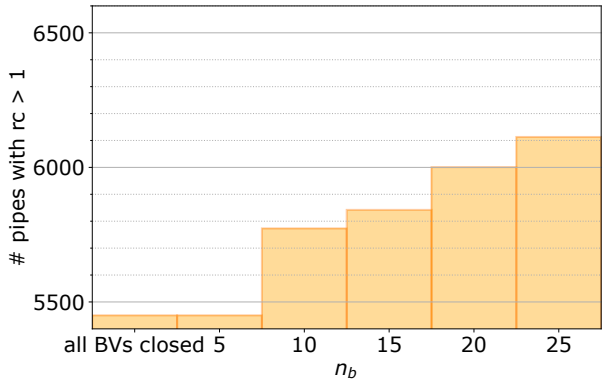

Fig. 7. Histogram representing the number of links with reserve capacity greater than 1 for all BVs closed, $n_b = 5, 10, 15, 20, 25$.

V. Conclusions and Future Work

This paper investigates the design-for-control (DfC) problem of optimal link addition and pressure control to improve the resilience of existing WSSs while minimizing the impact on network performance. We propose a mathematical programming formulation resulting in a MINLP, which can be applied for the solution of general WSS rehabilitation or expansion problems, given a set of candidate links for addition. In this regard, future work could investigate strategies

to identify sets of candidate links based, for instance, on the well-connectedness of demand nodes or supply areas [43]. Our numerical experiments focus on the particular case of sectorised WSSs, where the set of candidate links for addition is limited to existing closed BVs.

In contrast to previous rehabilitation design studies in WSSs, we apply mathematical optimization methods and adapt a spatial branch-and-bound procedure from the literature (BB_0) to attempt to solve globally the design-for-control problem of optimal link addition and pressure management. We modify BB_0 to include iterative optimality-based bound tightening (OBBT) throughout the branch-and-bound procedure and implement a model reduction step to address size limitations posed by operational networks. The tailored algorithm (BB_{BT+}) was shown to perform better than the state-of-the-art MINLP solver SCIP and BB_0 for both network models considered. Despite a significant reduction in the total number of completed branch-and-bound iterations compared to BB_0, BB_{BT+} provided at least as good feasible solutions with twice to three times smaller optimality gaps, suggesting that, for the considered problem, the quality of the solution does not depend as much on the total number of branch-and-bound iterations as it does on the tightness of the MILP relaxations solved to produce the lower bounds.

Finally, we perform an a posteriori validation of the increase in resilience resulting from the addition of new connections with a critical link analysis (CLA), using reserve capacity. The analysis of the solutions found for Net25 and BWPnet shows that opening BVs between DMAs increases the number of DMA inlets and independent supply paths, mitigating the impact of the failure of links on exclusive supply paths. Moreover, the computed solution provides a low cost strategy to improve the resilience of sectorised WSSs, as the cost of opening existing BVs is negligible compared to installing new pipes. The numerical experiments however show that, for the considered case studies, improving resilience (by adding new links) and minimizing AZP are conflicting objectives. Future work could investigate the implementation of dynamic aggregation solutions, to improve network resilience while preserving the benefits of network sectorization (i.e. pressure management and leakage monitoring).

APPENDIX I
MATRIX OF BINARY CONSTRAINTS FOR SECTORISED WSSS

For the particular case of sectorised WSSs, the matrix of constraints A in (9) is defined as below, by incrementally adding lines corresponding to the constraints on the vector of binary variables z representing the opening of the boundary valves between DMAs. We define C, the set of network DMAs. Given DMA $c_i \in C$, we consider the set C_i of all neighbouring DMAs connected to c_i by a closed boundary valve. $\forall\, c_j, c_k \in C_i$, $V_{ij}, V_{ik} \subset E_{\text{CP}}$ are the sets of closed boundary valves connecting DMA c_i to DMAs c_j and c_k respectively. The condition to limit aggregation of DMAs to pairing results in the following constraints on z:

$$\forall l \in V_{ij}, \quad 0 \leq \sum_{m \in V_{ik}} z_m \leq 1 - z_l$$

$$\text{or, equivalently,} \quad \forall l \in V_{ij}, \quad 0 \leq \sum_{m \in V_{ik}} z_m + z_l \leq 1$$

This constraint is expressed for all l in V_{ij}, all c_k in C_i and all c_i in C, each new inequality producing the coefficients of a new line of matrix A.

ACKNOWLEDGMENT

The authors acknowledge the financial support of EPSRC (EP/P004229/1, Dynamically Adaptive and Resilient Water Supply Networks for a Sustainable Future), EPSRC CDT in Sustainable Civil Engineering and Suez for conducting this research. The authors would also want to thank Kevin Henderson and Frank Van Der Kleij (Bristol Water) for sharing both the hydraulic model for the case study used in this research and their operational experience.

REFERENCES

[1] N. Jayaram and K. Srinivasan, "Performance-based optimal design and rehabilitation of water distribution networks using life cycle costing," *Water Resources Research*, vol. 44, no. 1, pp. 1–15, 2008.

[2] T. D. Prasad, S.-H. Hong, and N. Park, "Reliability based design of water distribution networks using multi-objective genetic algorithms," *KSCE Journal of Civil Engineering*, vol. 7, no. 3, pp. 351–361, 2008.

[3] T. D. Prasad and T. T. Tanyimboh, "Entropy Based Design of "Anytown" Water Distribution Network," *Water Distribution Systems Analysis 2008*, vol. 41024, no. August 2008, pp. 1–12, 2009.

[4] A. Di Nardo and M. Di Natale, "A heuristic design support methodology based on graph theory for district metering of water supply networks," *Engineering Optimization*, vol. 43, no. 2, pp. 193–211, 2011.

[5] A. Di Nardo, M. Di Natale, G. F. Santonastaso, and S. Venticinque, "An Automated Tool for Smart Water Network Partitioning," *Water Resources Management*, vol. 27, no. 13, pp. 4493–4508, 2013.

[6] S. Alvisi and M. Franchini, "A heuristic procedure for the automatic creation of district metered areas in water distribution systems," 2014.

[7] S. Atkinson, R. Farmani, F. a. Memon, and D. Butler, "Reliability indicators for water distribution system design: Comparison," *Water Resources Planning and Management*, vol. 140, no. 2, pp. 160–168, 2014.

[8] A. Di Nardo, M. Di Natale, G. F. Santonastaso, V. G. Tzatchkov, and V. H. Alcocer-Yamanaka, "Performance indices for water network partitioning and sectorization," *Water Science and Technology: Water Supply*, vol. 15, no. 3, pp. 499–509, 2015.

[9] E. Creaco, M. Franchini, and E. Todini, "Generalized Resilience and Failure Indices for Use with Pressure-Driven Modeling and Leakage," *Journal of Water Resources Planning and Management*, vol. 142, no. 8, p. 04016019, 2016.

[10] D. Halhal, G. A. Walters, D. Ouazar, and D. A. Savic, "Water Network Rehabilitation with Structured Messy Genetic Algorithm," *Journal of Water Resources Planning and Management*, vol. 123, no. 3, pp. 137–146, 1997.

[11] G. A. Walters, D. Halhal, D. Savic, and D. Ouazar, "Improved design of "Anytown" distribution network using structured messy genetic algorithms," *Urban Water*, vol. 1, no. 1, pp. 23–38, 1999.

[12] B. A. Tolson, H. R. Maier, A. R. Simpson, and B. J. Lence, "Genetic Algorithms for Reliability-Based Optimization of Water Distribution Systems," *Journal of Water Resources Planning and Management*, vol. 130, no. 1, pp. 63–72, 2004.

[13] M. L. Agrawal, R. Gupta, and P. R. Bhave, "Reliability-Based Strengthening and Expansion of Water Distribution Networks," *Journal of Water Resources Planning and Management*, vol. 133, no. 6, pp. 531–541, 2007.

[14] R. Wright, E. Abraham, P. Parpas, and I. Stoianov, "Control of water distribution networks with dynamic DMA topology using strictly feasible sequential convex programming," *Water Resources Research*, vol. 51, no. 12, pp. 9925–9941, 2015.

[15] A. Lambert and J. Thornton, "The relationships between pressure and bursts a state-of-the-art update," *Water21 - Magazine of the International Water Association*, 2011.

[16] A. Fugenschuh and J. Humpola, "A Unified View on Relaxations for a Nonlinear Network Flow Problem," Tech. Rep. Technical Report, Zuse-Institute, Berlin, 2013.

[17] T. Ding, K. Sun, C. Huang, Z. Bie, and F. Li, "Mixed-Integer Linear Programming-Based Splitting Strategies for Power System Islanding Operation Considering Network Connectivity," *IEEE Systems Journal*, vol. 12, no. 1, pp. 350–359, 2018.

[18] S. Huang and V. Dinavahi, "A branch-and-cut benders decomposition algorithm for transmission expansion planning," *IEEE Systems Journal*, vol. 13, no. 1, pp. 659–669, 2019.

[19] C. Bragalli, C. D'Ambrosio, J. Lee, A. Lodi, and P. Toth, "Water Network Design by MINLP," *IBM Research*, vol. RC24495, 2008.

[20] A. Gleixner, H. Held, W. Huang, and S. Vigerske, "Towards globally optimal operation of water supply networks," *Numerical Algebra, Control and Optimization*, vol. 2, no. 4, pp. 695–711, 2012.

[21] C. D'Ambrosio, A. Lodi, S. Wiese, and C. Bragalli, "Mathematical programming techniques in water network optimization," *European Journal of Operational Research*, vol. 243, no. 3, pp. 774–788, 2015.

[22] F. Pecci, E. Abraham, and I. Stoianov, "Global optimality bounds for the placement of control valves in water supply networks," *Optimization and Engineering*, vol. 67, no. 1, pp. 201–223, 2018.

[23] P. Belotti, C. Kirches, S. Leyffer, J. Linderoth, J. Luedtke, and A. Mahajan, "Mixed-integer nonlinear optimization," *Acta Numerica*, vol. 22, no. 2013, pp. 1–131, 2013.

[24] R. Wright, I. Stoianov, P. Parpas, K. Henderson, and J. King, "Adaptive water distribution networks with dynamically reconfigurable topology," *Journal of Hydroinformatics*, vol. 16, no. 6, p. 1280, 2014.

[25] B. J. Eck and M. Mevissen, "Quadratic approximations for pipe friction," *Journal of Hydroinformatics*, vol. 17, no. 3, p. 462, 2015.

[26] F. Pecci, E. Abraham, and I. Stoianov, "Quadratic head loss approximations for optimisation problems in water supply networks," *Journal of Hydroinformatics*, vol. 19, no. 4, pp. 493–506, 2017.

[27] S. Vigerske and A. Gleixner, "SCIP: global optimization of mixed-integer nonlinear programs in a branch-and-cut framework," *Optimization Methods and Software*, vol. 33, no. 3, pp. 563–593, 2018.

[28] P. Belotti, J. Lee, L. Liberti, F. Margot, and A. Wächter, "Branching and bounds tightening techniques for non-convex MINLP," *Optimization Methods and Software*, vol. 24, no. 4-5, pp. 597–634, 2009.

[29] L. Liberti and C. C. Pantelides, "Convex Envelopes of Monomials of Odd Degree," *Journal of Global Optimization*, vol. 25, no. 2, pp. 157–168, 2003.

[30] P. M. Castro and I. E. Grossmann, "Optimality-based bound contraction with multiparametric disaggregation for the global optimization of mixed-integer bilinear problems," *Journal of Global Optimization*, vol. 59, no. 2-3, pp. 277–306, 2014.

[31] E. Todini, "Looped water distribution networks design using a resilience index based heuristic approach," *Urban Water*, vol. 2, no. 2, pp. 115–122, 2000.

[32] T. T. Tanyimboh and A. B. Templeman, "Calculating Maximum Entropy Flows in Networks," *The Journal of the Operational Research Society*, vol. 44, no. 4, p. 383, 1993.

[33] A. Di Nardo, M. Di Natale, C. Giudicianni, D. Musmarra, J. M. Varela, G. F. Santonastaso, A. Simone, and V. Tzatchkov, "Redundancy Features of Water Distribution Systems," *Procedia Engineering*, vol. 186, pp. 412–419, 2017.

[34] R. Wright, M. Herrera, P. Parpas, and I. Stoianov, "Hydraulic resilience index for the critical link analysis of multi-feed water distribution networks," *Procedia Engineering*, vol. 119, pp. 1249–1258, 2015.

[35] A. Ostfeld, "Optimal reliable design and operation of water distribution systems through decomposition," *Water Resources Research*, vol. 48, no. 10, pp. 1–14, 2012.

[36] Y. Bao and L. W. Mays, "Model for Water Distribution System Reliability," *Journal of Hydraulic Engineering*, vol. 116, no. 9, pp. 1119–1137, 1990.

[37] M. Tabesh, J. Soltani, R. Farmani, and D. Savic, "Assessing pipe failure rate and mechanical reliability of water distribution networks using data-driven modeling," *Journal of Hydroinformatics*, vol. 11, no. 1, pp. 1–17, 2009.

[38] Gurobi Optimization, "Gurobi Optimizer Reference Manual," 2017.

[39] A. Wachter and L. T. Biegler, "On the implementation of an interior-point filter line-search algorithm for large-scale nonlinear programming," *Mathematical Programming*, vol. 106, no. 1, pp. 25–57, 2006.

[40] J. Currie, D. I. Wilson., N. Sahinidis, and J. Pinto, "OPTI: Lowering the Barrier Between Open Source Optimizers and the Industrial MATLAB User," in *Foundations of Computer-Aided Process Operations*, vol. 24, p. 32, 2012.

[41] A. Gleixner, M. Bastubbe, L. Eifler, T. Gally, G. Gamrath, R. L. Gottwald, G. Hendel, C. Hojny, T. Koch, M. E. Lübbecke, S. J. Maher, M. Miltenberger, B. Müller, M. E. Pfetsch, C. Puchert, D. Rehfeldt, F. Schlösser, C. Schubert, F. Serrano, Y. Shinano, J. M. Viernickel, M. Walter, F. Wegscheider, J. T. Witt, and W. Jakob, "The SCIP Optimization Suite 6.0," Tech. Rep. 773897, ZIB, Berlin, 2018.

[42] T. Walski, D. Chase, D. Savic, W. Grayman, S. Beckwith, and E. Koelle, "Advanced Water Distribution Modeling and Management," in *Civil and Environmental Engineering and Engineering Mechanics Faculty Publications*, ch. 3, pp. 75–132, 2003.

[43] M. Herrera and E. Abraham, "A Graph-Theoretic Framework for Assessing the Resilience of Sectorised Water Distribution Networks," *Water Resources Management*, vol. 30, no. 5, pp. 1685–1699, 2016.